university of groningen

University Medical Center Groningen

University of Groningen

Liquid crystalline solutions of cellulose in phosphoric acid for preparing cellulose yarns

Boerstoel, H.

IMPORTANT NOTE: You are advised to consult the publisher's version (publisher's PDF) if you wish to cite from it. Please check the document version below.

Document Version
Publisher's PDF, also known as Version of record

Publication date:
2006

Link to publication in University of Groningen/UMCG research database

Citation for published version (APA):
Boerstoel, H. (2006). *Liquid crystalline solutions of cellulose in phosphoric acid for preparing cellulose yarns*. s.n.

Copyright
Other than for strictly personal use, it is not permitted to download or to forward/distribute the text or part of it without the consent of the author(s) and/or copyright holder(s), unless the work is under an open content license (like Creative Commons).

The publication may also be distributed here under the terms of Article 25fa of the Dutch Copyright Act, indicated by the "Taverne" license. More information can be found on the University of Groningen website: https://www.rug.nl/library/open-access/self-archiving-pure/taverne-amendment.

Take-down policy
If you believe that this document breaches copyright please contact us providing details, and we will remove access to the work immediately and investigate your claim.

Downloaded from the University of Groningen/UMCG research database (Pure): http://www.rug.nl/research/portal. For technical reasons the number of authors shown on this cover page is limited to 10 maximum.

Download date: 05-05-2023

4. Rheology of solutions of cellulose in phosphoric acid

H. Boerstoel, J.B. Westerink, H. Maatman

Abstract

Capillary rheometry was performed on solutions of cellulose in superphosphoric acid. The influence of cellulose concentration, temperature and shear rate was studied. At low shear rates viscosity maxima were found at concentrations of 7.6 and 11.4 % w/w at 25 and 48°C, respectively. These values are in good agreement with the critical concentrations for the onset of a liquid crystalline phase at these temperatures as determined optically. Linear Bagley plots were found in practically all cases, except at high shear rates for the cases where the solutions are near the isotropic to anisotropic phase transition. In those situations concave Bagley plots were observed at high shear rates. For solutions that are fully anisotropic in the quiescent state, power law behavior was observed at a power of approximately 0.5, over a wide shear rate range. Whereas for solutions near the phase transition extreme shear thinning was observed at low shear rates, at higher shear rates again a power of 0.5 was found, indicating the occurrence of a flow induced phase transition.

4.1 Introduction

In Chapter 3 a new solvent for cellulose was presented. It was demonstrated that cellulose can be dissolved very fast up to high concentrations to form liquid crystalline phases in superphosphoric acid. Liquid crystalline solutions are good precursors in the spinning of highly oriented yarns, e.g. poly (para-phenylene terephthalamide) (PpPTA, commercialized under the trade names Twaron® and Kevlar® by Akzo Nobel and DuPont, respectively), polybenzoxazole (PBO, Zylon® by Toyobo) and Poly{2,6-diimidazo[4,5-b:4',5'-e]pyridinylene-1,4-(2,5-dihydroxy)phenylene} (PIPD or "M5" by Akzo Nobel)[1]. For cellulose two high tenacity yarns, spun from anisotropic solutions, are known from the literature[2-4]. Therefore, the liquid crystalline solution of cellulose in superphosphoric acid would appear extremely suitable for the production of high tenacity yarns.

In spinning equipment all sorts of flow occur: the kneading and mixing devices display high shear rates; during transport in piping the shear rates are low and intermediate; in spinnerets high shear rates and intermediate elongational rates; and in the stretching zone of the air-gap there occur intermediate elongational rates. Rough estimates of the deformation rates during processing are presented in Table 4.1.

Liquid crystalline polymers often display a rather complex rheological behavior. For instance, it was observed that the cellulose solution could no longer be transported through the piping of the machine upon the cellulose concentration being lowered. In order to elucidate some of the effects encountered during the spinning process the rheological behavior of the solutions was investigated. The next Chapter describes the determination of the elongational viscosity and the

present Chapter the rheological behavior of isotropic and anisotropic solution of cellulose in phosphoric acid in a shear flow field is presented, use having been made of a capillary rheometer.

Table 4.1: Deformation rates in various parts of the spinning process.

Stage of the process	shear rate (s^{-1})	elongational rate (s^{-1})
extruder	10^3-10^4	
tubes	10^0-10^2	
filters	10^1-10^2	
spinneret	10^4-10^6	10^2-10^3
air gap		10^2-10^3

4.2 Flow behavior of liquid crystalline materials

The rheology of liquid crystalline materials is often peculiar: the flow behavior is highly anisotropic, which manifests itself in the fact that five so-called Miesovicz viscosities and three Frank elastic constants are needed to describe the response of the material in the various directions[5]. In steady state shear flow different regimes can be distinguished. Depending on the shear rate, various degrees of shear thinning can be discerned, expressed in different power law coefficients. Onogi and Asada defined 2 shear thinning regions, with in between a Newtonian regime; the transitions were related to changes in the domain structure of the liquid crystalline material[6]. For various systems three regimes were also found experimentally[7]. The shear viscosity as a function of concentration often displays a maximum, corresponding to the isotropic to nematic phase transition, e.g., as described by Kwolek for poly (p-benzamide) in hydrofluoric acid[8]. The most important experimental observations were reviewed by Moldenaers[9].

Much attention was paid to two theories for the dynamics of liquid crystalline solutions. The one theory is a phenomenological description, based on continuum mechanics, known as the Leslie-Ericksen theory. The constitutive equation contains 6 viscosities, 5 of which are independent, as well as the three Frank elastic constants[7]. From the Miesovicz viscosities the Leslie-Ericksen coefficients can be determined. The Leslie-Ericksen approach gives rise to several conclusions. Firstly, flow alignment in simple shear is predicted, which means that the director is at a small angle with the axis of flow. Secondly, the apparent viscosity depends on the instrumental geometry. Unfortunately, the theory does not describe the shear thinning behavior[7].

The second theory is based on a molecular point of view of Doi and Edwards[10-14]. They describe the dynamics of solutions of rodlike macromolecules with a length L and a diameter d. A classification was made into various regimes: dilute, semidilute, and concentrated solutions, as indicated in Figure 4.1[10-14].

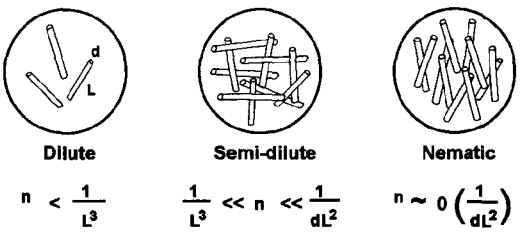

Figure 4.1: Doi and Edwards classification of concentration regimes for long rigid rods in solution[10-14].

The shear viscosity for the different regions was based on a molecular point of view. In a very dilute solution ($n<<1/L^3$) the Brownian motion of the molecules is independent. The viscosity η is a function of the solvent viscosity η_s, the number density n and the length L of the rods:

$$\eta \approx \eta_s(1+nL^3) \tag{4.1}$$

The increase in viscosity due to the rods is small in relation to the viscosity of the solvent. In the semi-dilute region ($1/L^3<<n<<1/dL^2$) the rods are strongly entangled but still in the isotropic state. The viscosity of this system is given by:

$$\eta = \eta_s(1+nL^3)^3 \tag{4.2}$$

Here, the viscosity is largely influenced by the presence of the rods and as $n>>1/L^3$, the viscosity is proportional to the concentration to the third power. Whereas in the dilute region the behavior is Newtonian, the viscosity in the concentrated regime is very much dependent on the deformation rate.
The nematic phase is obtained when the concentration is of the order of $1/dL^2$. The viscosity is not only dependent on molecular dimensions, but also on the order parameter S and hence on the deformation history:

$$\eta \propto n^3 M^6 f(S) \tag{4.3}$$

where M is the molecular weight of the rigid rods and f(S) a strongly decreasing function of the orientation. In practice the polymers are longer than the persistence length, which reduces the power in the molecular weight.

The Doi theory says that in slow shear flows the increase in orientational order is determinative of the decrease in viscosity above the critical concentration for the formation of a nematic phase. The systems are strongly shear thinning, due to induced orientation. Figure 4.2 presents the concentration and shear rate dependence of the viscosity as predicted by the Doi theory[14]. A shortcoming of the Doi theory is that due to an improved orientation the viscosity persistently decreases with concentration, whereas in practice the viscosity will increase again at higher concentrations.

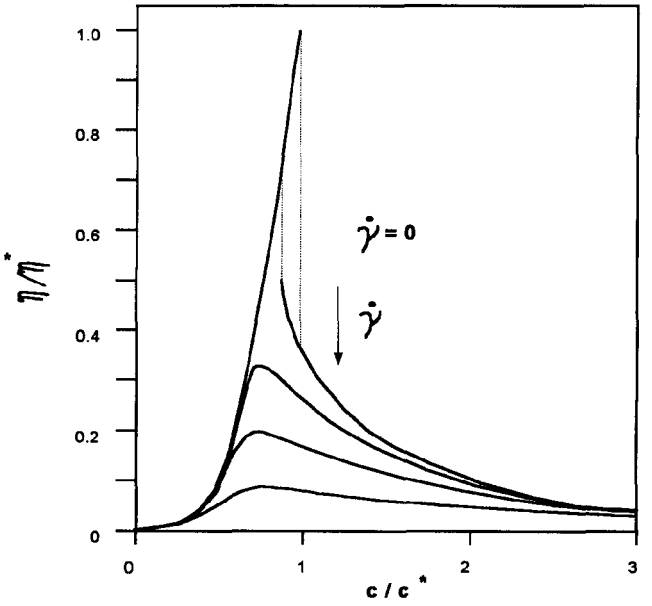

Figure 4.2: Concentration dependence of the steady state viscosity at various shear rates according to Doi and Edwards. The parameter c is the critical concentration, and η* is the viscosity at the critical concentration.*

Whereas in principle these theories relate to monodomains, it is now known that a number of properties are due to the presence of a polydomain flow[15]. Scaling concepts which incorporate the understanding of the flow behavior on a molecular level of the aforementioned treatments, have been used to account for the polydomain properties. An overview of the basic ideas has recently been published by Marrucci and Greco[16].

Kramers in 1946 already suggested that a flow field could be regarded as an equilibrium condition, in spite of the flow, by considering the velocity field as a potential[17]. Marrucci in 1977 used this idea to describe the effect of an extensional flow field on the phase equilibria of

rodlike molecules by modification of Flory's theory[18]. It was predicted that the critical concentrations shift to lower concentrations in the presence of an extensional flow field. This still accounts for a sudden phase transition. Mansuripur carried out calculations of the order parameter in a Maier-Saupe approach in the presence of elongational flow and proposed that the abrupt transition disappears above a critical deformation rate[19]. Weyland demonstrated that in the spinning of PpPTA from solutions in sulfuric acid no discontinuity was observed in the mechanical properties as a function of concentration, indicating that flow causes the transition from isotropic to anisotropic to vanish[20].
Mead and Larson carried out calculations based on Doi's theory[21]. They also concluded that a liquid crystalline state can be induced by shearing, resulting in a steep decrease of the viscosity with shear rate at this point. Navard and Haudin found experimentally that solutions of hydroxypropyl cellulose in acetic acid exhibited a more pronounced shear thinning behavior than in either the isotropic or the anisotropic state[22]. The flow curves were fitted by a power law, the index of which displayed a minimum in the vicinity of the phase transition.

4.3 Capillary rheometry

For a Newtonian fluid flowing through a capillary the wall shear rate γ_w depends on the volume flow rate Q and the radius R as:

$$\dot{\gamma}_w = \frac{4Q}{\pi R^3} \tag{4.4}$$

whereas the wall shear stress is given by:

$$\tau_w = \frac{4Q\eta}{\pi R^3} \tag{4.5}$$

with the shear viscosity η. For a power law fluid, with the following flow characteristic:

$$\tau = k\dot{\gamma}_w^{\,n} \tag{4.6}$$

the apparent wall shear rate is, analogous to Equation 4.4 :

$$\dot{\gamma}_{wa} = \frac{4Q}{\pi R^3} \tag{4.7}$$

The real wall shear rate relates to the apparent wall shear rate as:

$$\dot{\gamma}_w = \dot{\gamma}_{wa} \frac{3n+1}{4n} \tag{4.8}$$

The wall shear stress depends on the apparent wall shear rate as:

$$\tau_w = k \dot{\gamma}_{wa}^{\ n} \left(\frac{3n+1}{4n} \right)^n \tag{4.9}$$

where n is the power law coefficient; the term in parentheses is often referred to as the Rabinowitsch correction. Liquid crystalline systems often have various flow regimes with different power law coefficients.

The above reasoning holds for a stationary flow in the capillary, which means that no entrance or exit effects are taken into account. In practice, however, the capillary has a finite length, which is why end effects should be considered. In the entrance zone the velocity profile must settle to a stationary situation, an elongational flow field occurring in this region. The entrance pressure drop is determined by the geometry of the die entrance and is therefore independent of the ratio of capillary length to radius. At the exit of the capillary during the transportation of polymer melts or solutions, the pressure is often higher than the ambient pressure. The effect is related to the recoverable elastic energy, which is stored in the melt and manifests itself in a die swell. The end effects (both entrance and exit) can be compensated for by making a Bagley plot, i.e. by plotting the pressure versus the ratio of capillary length to radius, the intercept incorporating both the entrance and exit pressure drop, although the latter is often neglected . Bagley plots are mostly linear, and from the slope the shear stress at the wall can be determined:

$$\Delta p_{tot} = 2\tau_w \frac{L}{R} + \Delta p_e \tag{4.10}$$

where the intercept Δp_e , here called the end pressure, is the combined entrance and exit pressure drop[23,24].

Bagley plots are usually linear, but there are exceptions, e.g. due to viscous dissipation and fluid compressibility. For liquid crystalline polymers there might be even more causes for non-linear Bagley plots, e.g. the elongational flow field in the entrance zone may induce an orientation that could be lost in the shear flow of the capillary. This leads to concave Bagley plots[25].

Another effect in the capillary flow of liquid crystalline materials is that the wall may induce orientation. This is especially the case for low molecular weights, but may also occur in

polymeric systems. This effect leads to geometry dependent viscosities, which means that when use is made of capillaries with various radii, the flow curves do not connect. The instrumental geometry dependence of the viscosity is also predicted by the Leslie-Ericksen theory[7].

4.4 Experimental

4.4.1 Equipment

Most commercially available rheometers are not quite suited for the kind of solutions used in spinning highly oriented yarns. The reason for that is twofold. Firstly, the solvents utilized are strong acids, which require special materials; secondly, if measurements are carried out above room temperature, the entire reservoir will generally be heated, which might cause severe degradation during the measurements, due to the sensitivity to hydrolytic degradation of the polymers in the acid environment. Therefore, a capillary rheometer was constructed by adapting a plunger type of spinning machine.

The set up for the measurements is sketched in Figure 4.3. The container was filled by sucking the solution into it with a vacuum pump. The vessel was cooled by passing cold tap water through the double wall. By means of a plunger the solution was pressed through a multiflux heater in which the solution was brought to the desired temperature. Below the multiflux a measuring device was installed for measuring temperature and pressure, the latter being recorded by a Dynisco 5 M (0-200bar). Under it the capillary was installed in a housing.

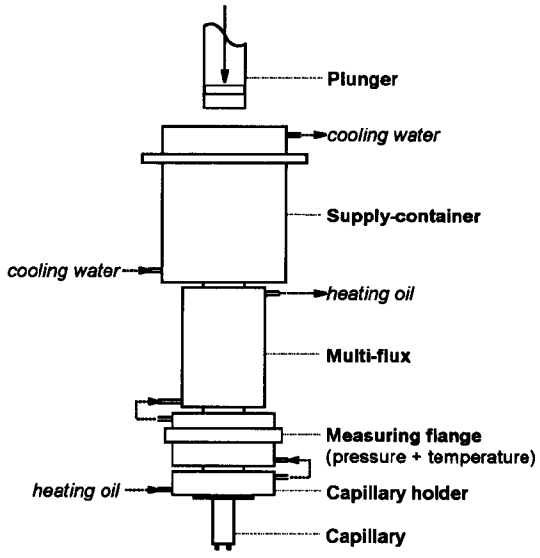

Figure 4.3: Capillary rheometer

Capillaries were used with radii of 0.25, 0.5, and 1.0 mm in order to cover a broad range of shear rates. For the construction of Bagley plots use was made of capillaries having lengths of 10, 20, 30, and 40 mm. The capillaries with a length of 10 and 20 mm were set in solid copper. The copper provides for good heat conduction from the housing, which is thermostated by circulating heated oil through it to the capillary. The longer capillaries were brazed into a hollow casing. Around the capillary water could be pumped to provide for a uniform temperature throughout the capillary. The experiments were performed at 25° and 39°C at various flow rates. Some additional experiments were carried out at 48°C.

4.4.2 Solution preparation

Cellulose V60 (DP 820) had been supplied by Buckeye, orthophosphoric acid by La Fonte Electrique SA, Bex Suisse (crystallized, 99% H_3PO_4) and polyphosphoric acid by Stokvis (84 % w/w P_2O_5). Solutions were prepared in two Z-kneaders: a W&P Luk Kneader (2.5 l) and a Linden Z-kneader (25l).

Orthophosphoric acid and polyphosphoric acid were mixed and heated at a temperature of approximately 45°C for at least 30 minutes to melt all the orthophosphoric acid and to equilibrate the acid mixture to some extent. This presolvent with a P_2O_5 content of approximately 74.4 % w/w was supercooled to approximately 10°C, followed by adding cellulose with an equilibrium moisture content of 5 % w/w. The definitions of solvent and presolvent are discussed in Chapters 2 and 3. The solutions were mixed for approximately 30 minutes. During mixing, the temperature rose to about 25 °C. An overview of the solutions is given in Table 4.1. Prior to use the solutions were stored at -18°C.

Table 4.1: List of solutions for capillary rheometry. The cellulose concentrations have been corrected for the equilibrium moisture content.

Solution	cellulose conc. (% w/w)	Clearing temperature (°C)
A	5.7	
B	7.6	28
C	8.6	31*
D	9.5	35*
E	10.5	40*
F	11.4	45
G	13.3	55
H	15.2	62
I	19	80*

* *Interpolated values from Chapter 3*

4.5 Results and discussion

4.5.1 Influence of concentration at low shear rates

For one capillary geometry the total pressure drop is plotted as a function of concentration at a temperature of 25° and 48 °C in Figure 4.4 , both lines displaying a maximum as a function of concentration. At 25°C the maximum appears at a concentration of approximately 8 % w/w cellulose. According to Doi's theory and to experimental findings by Kwolek the maximum represents the onset of an anisotropic phase. This means that the maximum corresponds to the maximum concentration at which the entire system is isotropic, or to the concentration having a clearing temperature of 25°C. From Figure 3.4 we learned that this critical concentration is in the same range. The minimum occurs around 11 % w/w cellulose. The observed rise in viscosity above 11 % w/w is not predicted by the Doi theory. At 48°C the maximum shifted to approximately 11 % w/w, and from microscopic observations the critical concentration at 48°C was approximately 12 % w/w, which is again in good agreement with the rheological data. The minimum at 48 °C shifted to approximately 15 % w/w.

Bagley plots of the series of concentrations were constructed for various shear rates for the series of concentrations and in all cases rather straight lines were observed. From the Bagley plots the wall shear stress was determined as a function of the apparent wall shear rate

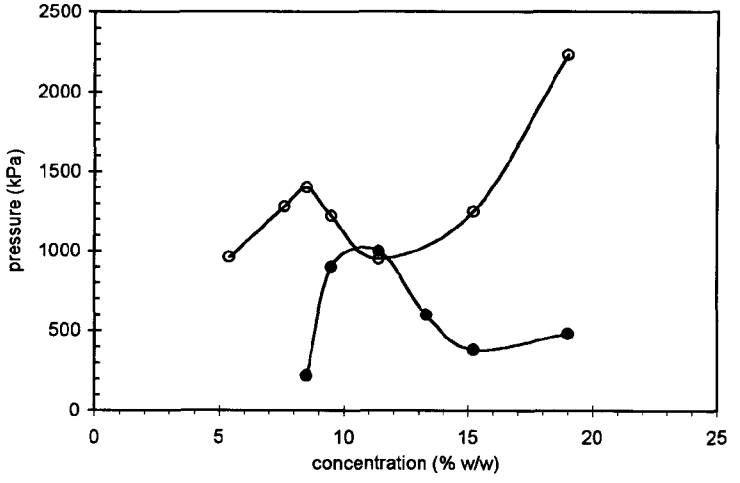

Figure 4.4: Pressure drop as a function of cellulose concentration, capillary length 40 mm, radius 1mm for an apparent wall shear rate of 30 s^{-1}, open circles 25°C, solid circles 48°C.

In Figure 4.5 the apparent viscosity, defined as:

$$\eta_{app} = \frac{\tau_w}{\dot{\gamma}_{wa}} \tag{4.11}$$

is plotted.

A maximum apparent viscosity is observed near 8 % w/w of dry polymer content. Above that concentration the viscosity decreases, and at low shear rates the viscosity continues to decrease even up to the highest concentrations. This effect is predicted by Doi's theory, although in experimental studies it is often found that after a maximum and a minimum the viscosity increases with increasing concentration, as it does here for the higher shear rates. In this system the maximum is not very pronounced, which is probably due to the large rheological forces and the long relaxation times of the polymer, as a result of which flow induced orientation is easily achieved. The viscosity of the solvent is already rather high, viz. approximately 0.4 Pas at 20°C[26], besides, the contour length of the cellulose molecule far exceeds the persistence length. In this case use was made of a cellulose with a DP of 820, corresponding to an average contour length of 4500 Å, which is at least fifteen times the persistence length. This means that although cellulose dissolved in phosphoric acid must have a rather extended conformation, the high molecular weight leads to the molecule having to be considered semiflexible. The macromolecular character probably causes differences between isotropic and anisotropic solutions to be leveled out to a certain extent.

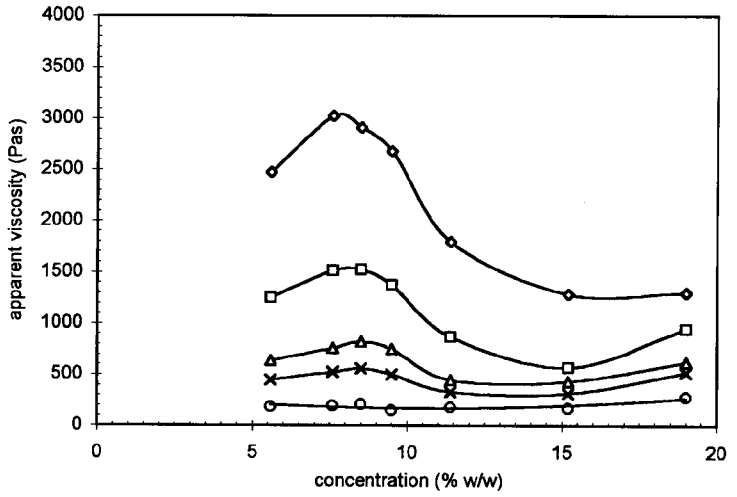

Figure 4.5: Apparent viscosity as a function of cellulose concentration at 25 °C using 1 mm capillaries for apparent wall shear stresses of 4, 8, 16 24 and 64 s^{-1}, respectively (downwards)

The relative height of the maximum, i.e., with respect to the viscosity at other concentrations, decreases with increasing shear rate. This may be ascribed to flow induced orientation and is in accordance with Doi's theory. At the highest apparent wall shear rate, which is used here, only a slight maximum is left. We must bear in mind that by definition the value of the apparent wall shear rate is the wall shear rate that would occur if a parabolic velocity profile were present; however, near the phase transition we are probably dealing with more or less plug flow, which means that near the wall the "real" shear rate is much higher and accounts for the induced orientation. The bulk is still unaffected, however.

Figure 4.6 shows the end pressure as a function of concentration. Here a local maximum is observed at the same concentration, as was the case for the viscosity. But above 11 % w/w the end pressure steadily increases with concentration. The end pressure is probably mainly caused by the elongational flow field in the entrance zone. This implies that although in the range above 11 % w/w the shear viscosity does not change much, the elongational viscosity increases considerably with concentration. Evidence is given in Chapter 5, where the elongational viscosity is presented as a function of concentration.

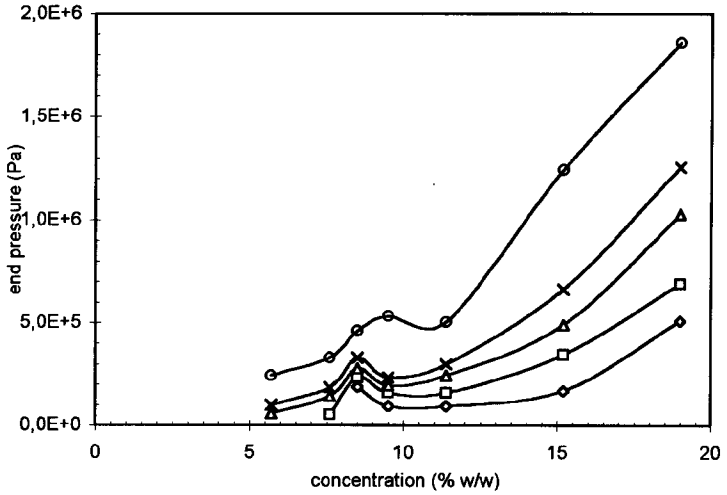

Figure 4.6: End pressure as a function of cellulose concentration at various apparent wall shear rates: 4, 8, 16, 24, 64 s^{-1} (upwards)

4.5.2 Influence of shear rate

The effect of an enhanced shear rate on viscosity was studied at 25 °C for 7.6, 11.4 and 15.2 % w/w, the last two concentrations also having been investigated at 39°C. It is found that if the solutions is in a true anisotropic phase, the Bagley plots are all rather linear, even for the

highest shear rates. However, in the case of the solution with a cellulose concentration of 7.6 % w/w very concave curves are observed for the high shear rates. This might be caused by the induced orientation in the elongational flow field, slowly relaxing in the shear flow field in the capillary, as indicated by Vermant[25]. Bagley-plots for a 7.6 % w/w and a 15.2 % w/w solution are shown in Figure 4.7.

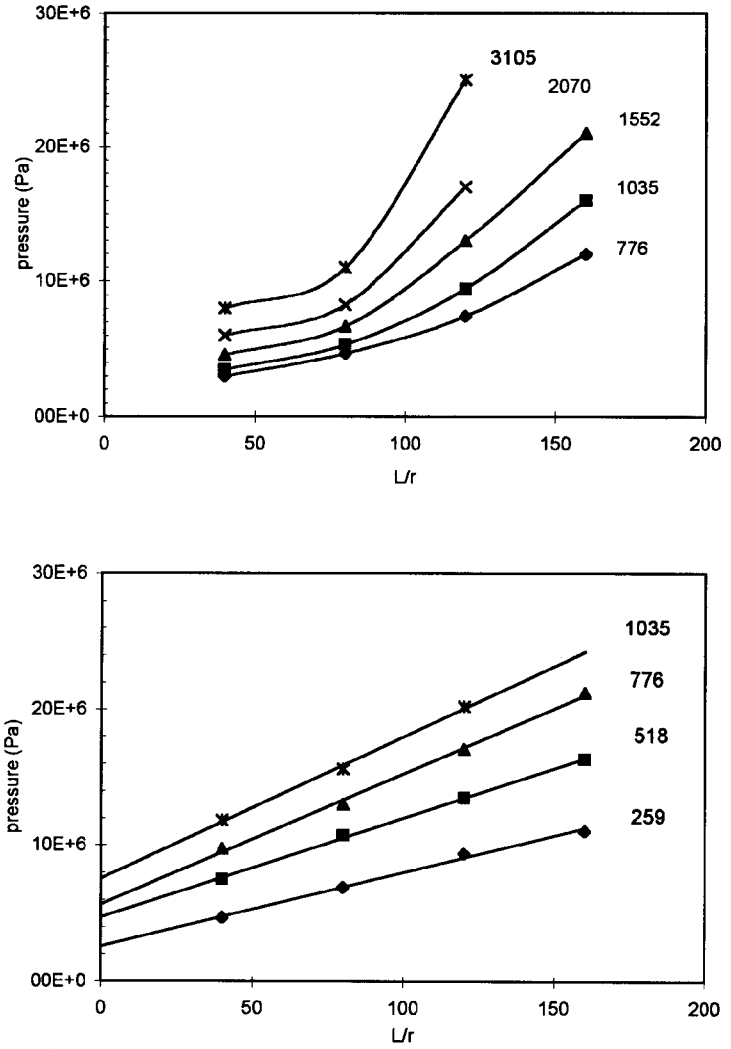

Figure 4.7: Bagley plots for 7.6 % w/w (top) and 15.2 % w/w (bottom) cellulose solutions at 25°C, using 0.25mm radius capillaries, apparent wall shear rates as indicated

At 39°C concave Bagley plots are found for 11.4 % w/w at the higher shear rates. In the other cases rather straight lines are observed. At this temperature this solution is close to the clearing temperature. In Figure 4.8 the wall shear stress is plotted versus the apparent wall shear rate for 3 concentrations at room temperature using all three diameters of the capillaries to cover a wide range of shear rates. For this graph only those cases were used which yielded linear Bagley plots. Several strange phenomena can be noticed.

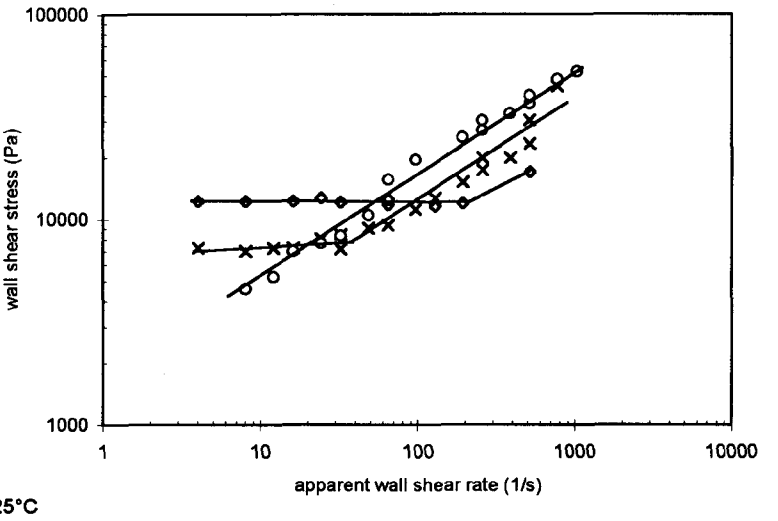

Figure 4.8: Wall shear stress as a function of apparent wall shear rate at 25°C for 7.6 % w/w (diamonds), 11.4 % w/w (crosses) and 15.2 % w/w (circles) cellulose solutions

Firstly, the curves for the different capillary widths do not connect completely, though the differences are not large. This was also found for Vectra®, a thermotropic polyester, and was ascribed to differences in orientation across the capillary width and to entrance effects[25]. However, the effect is not unduly great here and for the determination of the flow parameters the difference between the various capillary widths was disregarded.

Secondly, a change in slope was observed for a number of cases. For a solution containing 15.2 % w/w cellulose, which is far above the critical volume fraction, the wall shear stress versus the apparent wall shear rate yields a straight line on a log-log scale. This implies that in this range of shear rates there occurs no change of mechanisms. The three regions in the flow curve defined by Onogi and Asada were not found. Probably, due to the high viscosities only the third regime was observed here. The 11.4 % w/w solution initially has a constant shear stress value. Above an apparent wall shear rate of approximately 30 s^{-1} a shear rate dependent shear stress is observed, the line running approximately parallel to the curve of 15.2 % w/w.

For the 7.6 % w/w solution the plateau value of the wall shear stress is also followed by a shear rate dependent shear stress. Although only a single point seems to support this idea, it fits in with the results for the other solutions.

It therefore seems that near the equilibrium phase transition there is some kind of yield stress, which can also be regarded as extreme shear thinning behavior. Navard and Haudin also observed that solutions near the phase transition were far more shear thinning than the isotropic or the anisotropic phase[22]. A shear induced phase transition to the anisotropic phase occurs above a critical shear rate, which is naturally concentration dependent. Above this critical wall shear rate no difference in flow behavior is observed with the fully anisotropic solutions. The deformation induced phase transition is considered to be caused by the shear flow in the capillary; however, it might just as well be caused by the elongational flow field in the entrance zone of the capillary. For convenience we use a critical shear rate rather than a critical elongational rate, because of the fact that the elongational flow field in the entrance zone is unknown. Moreover, the critical apparent wall shear rate is merely a fictitious value; throughout the capillary there is a wide range of shear rates.

Figure 4.9 presents the flow curves of the 11.4 and 15.2 % w/w at 39°C. The same phenomena are found. Whereas the 15.2 % w/w solution still displays the same flow behavior over the entire shear rate range, the 11.4 % w/w solution shows a deformation induced anisotropic phase above a critical apparent wall shear rate of approximately 250 s^{-1}.

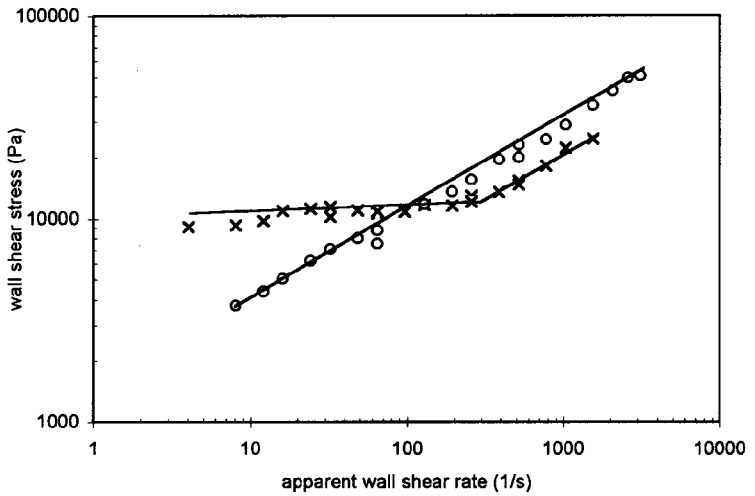

Figure 4.9: Wall shear stress as a function of apparent wall shear rate at 39°C for 11.4 % w/w (crosses) and 15.2 % w/w (circles) cellulose solutions

The shear rate dependent parts of the flow curve were fitted by a power law. The results are displayed in Table 4.2. In addition, mention is made of the critical apparent wall shear rates, if determined

Table 4.2: Power law coefficients and critical apparent wall shear rate for a number of concentrations and temperatures

cellulose content (% w/w)	T (°C)	$\gamma_{wa,cr}$ (s^{-1})	k ($\left(\frac{3n+1}{4n}\right)^n$ Pa)	n (-)
7.6	25	200		
11.4	25	30	1300	0.5
15.2	39		1550	0.5
11.4	39	250	1500	0.4
15.2	39		1450	0.4

4.6 Conclusions

Capillary rheometry was performed on solutions of cellulose in phosphoric acid which were either in the vicinity of the critical concentration for an anisotropic phase or clearly above that concentration. In practically all cases linear Bagley plots were found. Some deviations were found only near the phase transition at the highest shear rates. At low shear rates a maximum viscosity was found, as predicted by Doi's theory and observed for other systems in many occasions. The concentration at which this maximum appeared was in good agreement with the critical concentration determined by polarization microscopy.

For concentrations well above the critical concentration the flow behavior could be fitted by a power law. There was no difference between various flow regimes, as described by Onogi and Asada[6] . Instrumental geometry was found to have a small influence.

In the proximity of the phase transition in the quiescent state a plateau value for the shear stress was found, which can also be described as an extremely shear thinning flow behavior. This effect might be ascribed to flow induced orientation in the wall layer serving as a lubricant, the thickness of which varies with the shear rate. Above a critical shear rate the shear stress depends on the shear rate in the same fashion as in the case of the clearly anisotropic solutions, which is why it was concluded that there occurred a flow induced phase transition. A critical apparent wall shear rate could be indicated, though this is merely a relative value. For, the real shear rate varies across the width of the capillary; moreover, there might be a contribution of the elongational flow field above the capillary.

4.7 Acknowledgment

The authors wish to thank Mr. R. Willemsen for the practical support.

4.8 References

1. D.J. Sikkema, V.L. Lishinski, WO 9425506 (Akzo Nobel)
2. J.P. O'Brien, US 4464323 (DuPont)
3. J.P. O'Brien, US 4501886 (DuPont)
4. P. Villaine, C. Janin, WO8505115 (Michelin)
5. S.J. Picken, "Orientational order in aramid solutions", Ph. D. Thesis Utrecht (1990)
6. S. Onogi, T. Asada in "Rheology" eds G.Astarita, G. Marrucci, L. Nicolais,Vol. 1 421 (1980)
7. K. Wissbrun, J. Rheology **25**, 619 (1981)
8. S.L Kwolek NL6908984 (DuPont)
9. P. Moldenaers in "Rheology and processing of liquid crystal polymers"(eds. D. Acierno and A.A Collyer), Chapman &Hall
10. M. Doi, S.F. Edwards, J.Chem. Soc. Faraday Trans.II **74**, 568 (1978)
11. M. Doi, S.F. Edwards, J.Chem. Soc. Faraday Trans.II **74**, 918 (1978)
12. M. Doi, J. Pol. Sci., Pol. Phys ed. **18**, 2055 (1980)
13. M. Doi, J. Pol. Sci., Pol. Phys ed. **19**, 229 (1981)
14. M. Doi, S.F. Edwards, "The theory of polymer dynamics", Oxford Science Publications, Clarendon Press, Oxford (1986), Chapter 10
15. F. Beekmans, "Rheology and changes in structure of liquid crystalline polymers", Ph. D. Thesis Delft (1997)
16. G. Marrucci, F. Greco, in "Advances in Chemical Physics" (I. Prigogine and S. Rice eds), Wiley, New York (1993), pp 331-404
17. H.A. Kramers, J. Chem. Phys.**14**, 415 (1946)
18. G. Marrucci, A. Ciferri, Polymer Lett. Ed. **15**, 643 (1977)
19. M. Mansuripur, Int. J. Multiphase Flow **9(3)**, 299 (1983)
20. H.G. Weyland, Polym. Bull. **3**, 331 (1980)
21. D.W. Mead, R.G. Larson, Macromolecules **23**, 2524 (1990)
22. P. Navard, J.M. Haudin, J. Pol. Sci. , Pol. Phys. Ed. **24**, 189 (1986)
23. R.B. Bird, R.C. Armstrong, O. Hassager, "Dynamics of polymeric liquids" vol1 Fluid Mechanics, 2nd ed. Wiley, New York (1987)
24. C.D. Han, "Rheology in polymer processing", Academic press, New York (1976)
25. J. Vermant, "Flow-induced structures and rheology of liquid crystalline polymers", Ph. D. Thesis Leuven (1996)
26. Kirk-Othmer, Encyclopedia of chemical technology, 4th ed, vol18, pp669, John Wiley , New York (1996)